5-axis CNC Micro-milling for Rapid, Cheap and Background Free NMR Micro-coils

Vincent Moxley-Paquette,[a] Daniel Lane,[a] Ronald Soong,[a] Paris Ning,[a] Monica Bastawrous,[a] Bing Wu,[a] Maysam Zamani Pedram,[bc] Md Aminul Haque Talukder,[b] Ebrahim Ghafar Zadeh,[b] Dimitri Zverev,[d] Richard Martin,[e] Bob Macpherson,[f] Mike Vargas,[f] Daniel Schmidig,[g] Stephan Graf,[g] Thomas Frei,[g] Danijela Al Adwan-Stojilkovic,[g] Peter De Castro,[g] Falko Busse,[h] Wolfgang Bermel,[h] Till Kuehn,[g] Rainer Kuemmerle,[g] Michael Fey,[i] Frank Decker,[h] Henry Stronks,[j] Ruby May A. Sullan,[k] Marcel Utz,[l] André J. Simpson[ak]*

a. Environmental NMR Center, University of Toronto Scarborough, 1265 Military Trail, Toronto, Ontario, Canada

b. Lassonde School of Engineering, York University, 4700 Keele St, North York, Ontario, Canada

c. Faculty of Medicine, Department of Radiology, University of British Columbia, Vancouver, British Columbia, Canada

d. NSCNC Manufacturing Ltd, 1515 Broadway St. Unit 607, Port Coquitlam, British Columbia, Canada

e. IMicrosolder, 57 Marshall St. West, Meaford, Ontario, Canada

f. Apogee Steel Fabrication Inc., 3600 Erindale Station Rd, Mississauga, Ontario, Canada

g. Bruker BioSpin AG, Industriestrasse 26, 8117 Fällanden, Switzerland

h. Bruker Biospin GmbH, Silberstreifen 4, 76287 Rheinstetten, Germany

i. Bruker Corporation, 15 Fortune Drive, Billerica, MA 01821-3991, USA

j. Bruker Canada Ltd, 2800 High Point Drive, Milton, Ontario, L9T 6P4

k. Department of Physical and Environmental Science, University of Toronto Scarborough, 1265 Military Trail, Toronto, Ontario, Canada

l. School of Chemistry, University of Southampton, Southampton SO17 1BJ, United Kingdom

*Corresponding Author – andre.simpson@utoronto.ca

ABSTRACT: The superior mass sensitivity of micro-coil technology in Nuclear Magnetic Resonance (NMR) Spectroscopy provides potential for the analysis of extremely small mass-limited samples such as eggs, cells, and tiny organisms. For optimal performance and efficiency, the size of the micro-coil should be tailored to the size of the mass-limited sample of interest, which can be costly as mass-limited samples come in many shapes and sizes. Therefore, rapid and economic micro-coil production methods are needed. One method with great potential is 5-axis Computer Numerical Control (CNC) micro-milling, commonly used in the jewelry industry. Most CNC milling machines are designed to process larger objects and commonly have a precision >25 µm (making the machining of common spiral micro-coils, for example, impossible). Here, a 5-axis MiRA6 CNC milling machine, specifically designed for the jewelry industry, with a 0.3 µm precision was used to produce working planar micro-coils, microstrips, and novel micro-sensor designs, with some tested on the NMR in less than 24 hours after the start of the design process. Sample wells could be built into the micro-sensor and could be machined at the same time as the sensors themselves, in some cases leaving a sheet of Teflon as thin as 10 µm between the sample and sensor. This provides the freedom to produce a wide array of designs and demonstrates 5-axis CNC micro-milling as a versatile tool for the rapid prototyping of NMR micro-sensors. This approach allowed the experimental optimization of a prototype microstrip for the analysis of two intact adult *Daphnia magna* organisms. In addition, a 3D volume slotted tube resonator was produced that allowed for 2D ^{1}H-^{13}C NMR of *D. magna* neonates and exhibited ^{1}H sensitivity (nLOD$_o^{600}$= 1.49 nmol s$^{1/2}$) close to that of double striplines, which themselves offer the best compromise between concentration and mass sensitivity published to date.

INTRODUCTION

The medical field have recently identified environmental exposure as the predominant cause of many neurodegenerative diseases including links to heavy metals, pesticides and other environmental factors,[1–4] however exact causes are still not clear. Similarly, in environmental research there is a need to better understand "why" chemicals are toxic.[5] Present

environmental policies are commonly based on apical endpoints such as death, movement and reproduction, but provide little information on sub-lethal impacts, toxic mechanisms or synergistic effects.[6,7] *In vivo* NMR is evolving as a powerful technique to help fill these gaps in knowledge.[8] The living organism arguably represents the "ultimate biosensor" responding in real-time to its environment, while the NMR spectrometer "interprets" the biochemical changes, providing information to help explain sub-lethal toxicity at the molecular level.[8–15]

In environmental research, understanding toxic impacts and responses in eggs and neonates from aquatic organisms is of paramount importance. For example, keystone species such as *D. magna* consume algae and are in turn eaten by fish.[16] As such, if they are impacted by a toxin and disappear, there is potential for the entire ecosystem to collapse. In times of environmental stress (low oxygen, cold temperature, lack of food, etc.) *Daphnia* reproduce sexually and produce resting eggs.[17] These are deposited into the sediments and can remain viable for decades (only hatching when ideal environmental conditions return).[17] In this way, the species can outlast environmental changes (winters, droughts, longer term climatic shifts, etc.). However, if anthropogenic toxins eradicate these reserve egg banks the implications could be catastrophic for the ecosystem.[17] Unfortunately, toxic impacts in "static" eggs are extremely challenging to study using conventional apical indicators such as death, movement, and reproduction. Similarly *D. magna* neonates (<24 hrs old) have been shown to respond differently to contaminants compared to adults[18] and thus more in depth molecular information is needed for this particularly at risk age group.

While NMR provides unique information as to the chemical composition of living systems, the small size of eggs and neonates make them very challenging to study using conventional 5 mm NMR probes**.**[15] However, micro-coil NMR offers vastly improved mass sensitivity (ideal for tiny specimens such as eggs).[19] Recently, Fugariu *et al.*[19] showed that matching the diameter of micro-coils to the sample of interest could increase signal by 100's, even 1000's of time. Given that eggs, neonates, and small organisms come in a range of shapes and sizes, for optimal NMR detection there is a need to develop a diversity of size-matched micro-coils in a rapid and cost-effective manner.

Single sided planar micro-coils and Helmholtz micro-coils are commonly produced through electroplating Cu onto a Cr/Au seed layer on a glass substrate (with a photoresist mould guiding the electroplating of the turns).[20–22] With some exceptions, mainly for research,[23–28] the vast majority of commercially available NMR micro-coils are made in clean rooms via multi-layer deposition[20,21,29–31] and while exquisitely precise, are expensive and time intensive to construct.

An alternative approach involves CNC micro-milling, which so far has been used to produce various larger planar NMR coils (11.1 mm to 17.1 mm)[32] as well as larger microstrip designs[27] that don't require micron-level precision to produce. However, the majority of CNC mills are made to process larger objects and commonly have a precision and repeatability of 25 µm or more, which makes the machining of spiral micro-coils that commonly have copper channels with spacings of 20-30 µm impossible.[19,20,29] Interestingly, the jewellery industry requires high precision to produce 3D objects (both for direct milling of jewellery and making castable moulds), and a range of high precision 5-axis micro mills were developed at reasonably affordable prices. For example, the mill used in this research has a precision of 0.3 µm and cost ~$40K USD to deliver and install (roughly analogous to 3-4 commercial micro-coils). The 5-axis CNC micro-milling technique discussed here has the capability to manufacture both planar and 3D volume micro-coils with much smaller dimensions and, to the authors knowledge, has yet to be applied within NMR micro-coil development.

Figure 1. The MiRA6 CNC milling machine (top, left) used in this study (photo used with written permission from NSCNC manufacturing LTD). This machine can handle milling bits down to 5 µm in diameter. An electron microscope image (bottom, left) of a Performance Micro Tool micron series milling bit next to a human hair (used with written permission from Performance Micro Tool). Examples of coils/sensors machined in this present study include a spiral coil[33] (top, middle, 16 turns with 40 µm wide copper and 60 µm spacing), as well as a microstrip[34] (centre, 3 mm length and 150 µm width). A sample well can also be milled as the coil is made with a thin PTFE membrane separating the coil from the sample (bottom, middle). Pins on the micro-coil and micro-sensors are inserted into contacts at the top of a modified Bruker TXI probe body (right). A microstrip is shown as an example and the z-gradient was intentionally moved to the side. The green arrow shows a hole within the custom gradient helping ensure proper positioning of the detection coil within the probe.

In this study, the feasibility of using both 3-axis and 5-axis CNC micro-milling in the production of working planar and 3D volume micro-coil/micro-sensor technology was tested. A series of previously published

planar micro-sensor designs[20,34] along with some novel designs were manufactured to demonstrate the capability of using CNC micro-milling for NMR micro-coil development. In addition, a series of microstrip designs[34] were optimized for analysing ^{13}C-labelled *D. magna* adults as well as a slotted-tube resonator (STR)[35] for the study of neonates. It was found that cavities and sample holders could be made from copper/Teflon sheet at the same time as the coils were made. As such, it was possible to simulate, mill, tune/match, and test micro-sensors on the NMR all within 24 hours, demonstrating the potential of 5-axis CNC micro-milling in rapid prototyping of micro-coil and micro-sensor technology.

EXPERIMENTAL METHODS

CNC Milling. All copper-plated Teflon (CuFlon®) used in this study was purchased from Crane® Polyflon and had a copper thickness of ½ Oz/ft^2 (~17.5 µm thick) as well as a PTFE dielectric thickness of 1/16" (~1.588 mm). The material is 100% PTFE dielectric with no fillers. Printed Circuit Boards using a 18 µm copper thickness were previously used to build extremely sensitive resonator designs.[27] All milling bits/drill bits that were used in this study (ET-5-1250-F, ET-5-0312-F, ET-4-0156-C, 100M2X300S, 50M2X150S, and KT-0200-R) were purchased from Performance Micro Tool. 3D models of each micro-coil/micro-sensor were constructed using Rhinoceros 5®. G-code Tool Paths were programmed using the plugin MadCAM® and executed via the NSControl software on the MiRA6 CNC milling machine.

For planar coils/sensors, the 3-axis mode of the MiRA6 was mainly used for milling, although the 4th axis and 5th axis were used to orient the part as needed.

The full 5-axis mode of the MiRA6 was used to mill a 3D volume STR design adapted from Benabdallah *et al.*[35] (with 0.8 mm spacing from a copper tube with a 1.270 mm O.D. and a 0.813 mm I.D.). To connect this STR to the rest of the probe network, an adapter was made from CuFlon®. This board contained groves with precise depths and pads that allowed the resonator to be accurately positioned and soldered in place. For this resonator, samples were placed in a thin walled glass capillary purchased from Hampton Research with either a 700 µm O.D./680 µm I.D. (Cat: HR6-164), 500 µm O.D./480 µm I.D. (Cat: HR6-160), or a 100 µm O.D./80 µm I.D. (Cat: HR6-152) and then inserted into the STR.

After milling, the milled resonators were tuned and matched using non-magnetic ceramic capacitors from American Technical Ceramics and Knowles (purchased from Digi-key). See Figure 1 for how the completed sensor connects with the rest of the modified Bruker TXI probe body. CNC milling and Simulation paramiters are described in greater detail within the Supporting Information.

NMR Experiments. All experiments were performed using a 500 MHz Bruker Avance III NMR Spectrometer and Topspin 3.5 pl7 was used for data collection. Data analysis was performed using both Bruker's Topspin 3.5 and ACD labs Spectrus Processor version 2018.1.1. NMR experimental paramiters, samples used (including biological samples), and methods for metabolite identification are described in detail within the Supporting Information.

RESULTS AND DISCUSSION

Demonstration of Planar Micro-coil and Micro-sensor Construction using CNC Micro-milling. To demonstrate the ability of CNC milling to produce micro-coils/micro-sensors, four single sided planar designs (two published and two unpublished) were milled using the 3-axis mode of the MiRA6. This included a 3 mm long and 150 µm wide microstrip that was adapted from Chen *et al.*[34] and a 1000 µm I.D. planar micro-coil that was adapted from Massin *et al.*[20]. Two novel designs (inspired by the microstrip[34] and micro-slot designs[36]) were also created to demonstrate the capability of micro-milling for rapid prototyping of new sensor designs. One design was an array of five parallel 0.2 mm wide strips (spaced 0.1 mm apart) with an overall length of 7 mm and overall width of 1.4 mm (named a "Parallel Array" here). The other design contained a staggered array of 0.5 mm long and 0.1 mm wide slots (spaced 0.2 mm apart) with an overall length of 7 mm and an overall width of 1.7 mm (termed a "Staggered Slot Array" here). All designs are illustrated in Figure 2 (left column).
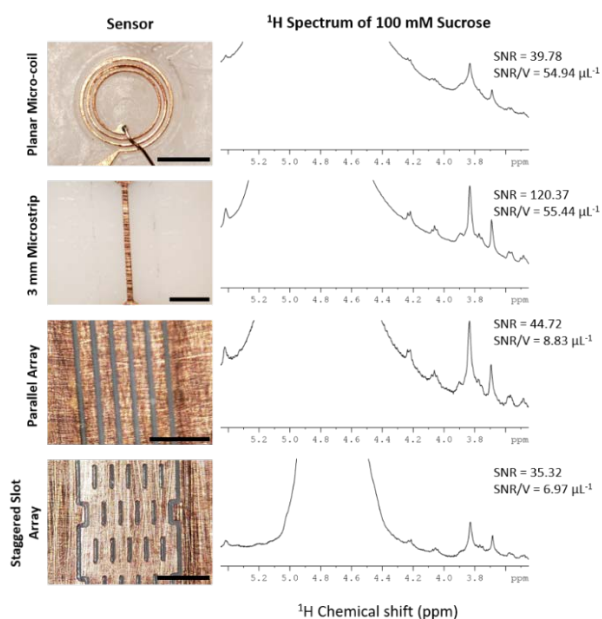

Figure 2. The micro-coil and micro-sensors produced using the 3-axis mode of the MiRA6 (left). Black bars are scaled to 1 mm. The images for the Parallel Array and the Staggered Slot Array were magnified intentionally to highlight the structural features. Each sensor was used to analyse a 100 mM Sucrose solution (in H$_2$O) within a 500 µm O.D. glass capillary with 10 µm walls (right, 256 scans).

Sample well design is considered in the next section, here to simply demonstrate the feasibility of NMR data collection a 500 µm O.D./480 µm I.D. capillary was filled with 100 mM Sucrose and secured over each coil/sensor. As shown in Figure 2 (right column), all sensor designs were able to obtain a ^{1}H NMR spectrum of Sucrose. The 3 mm microstrip provided the highest total SNR for the sucrose signal. When corrected for the volume of the sample over the active region, both the planar micro-coil and the 3 mm microstrip provided a similar SNR per µL of sample. This is consistent with the literature that has shown both these designs to be extremely sensitive.[30,34] The lineshape, however was slightly better for the 3 mm microstrip compared to the planar micro-coil. This is likely due to the length of coil/sample which in this case is much larger than the width (allowing for easier shimming using Z orientated shims systems).[37]

Although the Parallel Array and the Staggered Slot Array exhibited the worst SNR for sucrose, they provided the most sinusoidal nutation curves (see Figure S1), demonstrating that these designs have the most uniform B_1 field across the entire sample.[19] This is due to the Parallel Array and Staggered Slot Array having a larger excitation area than the planar micro-coil or 0.15 mm wide microstrip (thus the B_1 field penetrated the entire sample volume). Conversely, the much smaller microstrip and micro-coil excite only a smaller volume of the sample. These smaller coils show a reasonable "90°" pulse because as the pulse length is increased both the flip angle increases along with the penetration of the coils stray field further into the sample. However, as the pulse is increased further, spins far from the coils surface only receive a weak RF field (<50% of RF field strength compared to the coil surface) and thus do not undergo inversion leading to poor nutation performance. Indeed, this was reported previously when smaller coils were used to excite a much larger sample.[19] In summary, these introductory prototypes show that CNC micro-milling has potential for creating working micro-coils and micro-sensors for use in NMR spectroscopy.

Optimization of Sample Well Geometry. As mentioned previously, CNC milling can simultaneously create the sample well at the same time the micro-sensor is made. In the case of the CuFlon® material used here (pure PTFE coated with copper), this is advantageous as the sample holder/well can be machined directly into the PTFE layer (which has high chemical compatibility and no spectral background in ^{1}H NMR).[38] By making the PTFE layers between the sample and coil/sensor as thin as possible, filling factor and signal can be improved. Although the MiRA6 has a positioning resolution of 0.3 µm, a spindle runout (inaccuracies that cause a tool to deviate from the ideal axis) of ~1 µm remains an issue. Therefore, in theory it should be possible to machine down to PTFE layers approaching 2 µm. However, in practice the PTFE tends to tear from the shear forces exerted from the milling bit when it gets extremely thin

as well as the remaining PTFE membrane becoming easily ruptured during everyday use. As such, we have found a Teflon thickness of 10-30 µm to be the best compromise for robust manufacturing and good SNR while being sturdy enough for everyday use.

With the ability to create the sample wells using 5-axis milling it is possible to create various size and shaped wells to optimize signal. To demonstrate this, three microstrips (3 mm length and 0.15 mm width) were milled each having a different well design/shape. One was a 500 µm diameter capillary well that was drilled from the top of the sensor down to the bottom of the strip (behind the strip), leaving a 10 µm PTFE layer between the sample and the strip. Another design had a 2 mm x 3 mm rectangular well and the third design had a 3 mm diameter circular well, both milled from the back so the wells were directly behind the strip (see Figure 3). For both the circular and rectangular designs, the larger surface area of the thin membrane made it difficult to mill to 10 µm thickness. Instead, a 30 µm PTFE layer between the sample and the strip was left which could be reproducibly matched without tearing. As shown in Figure 3B/C (middle column), the Teflon is so thin after machining the microstrips can be seen through the membrane from the back of the device.

A 100 mM Sucrose solution in H_2O was used to test the sensors' performance. As shown in Figure 3, the microstrip with the capillary well provided the best lineshape in part due to the long thin vertically oriented sample being most amenable to shimming[37] as mentioned above. Magnetic susceptibility distortions introduced by the wider shape of the sample[39] also likely contributed. In this case the sample is introduced directly into the Teflon channel and an additional glass capillary is not required. The round and rectangular sample wells (Figure 3B and 3C respectfully) provided a reduced lineshape but are still important designs as they match the size of many small aquatic organisms. In turn, as the ^{1}H lineshape for living organisms is relatively wide (rarely less than ~50 Hz, ~0.1 ppm at 500 MHz)[9] due to magnetic susceptibility distortions, 2D ^{1}H-^{13}C NMR is commonly required for the discrimination of metabolites.[13,14] Indeed, the lineshape for the square and round well for sucrose is ~25-50Hz (already better than the natural lineshape of intact organisms). As such, while the capillary well will have clear advantages for dissolved homogeneous samples, the round and rectangular well designs would work for inhomogeneous living samples such as *D. magna* or *Hyalella azteca* (commonly used for toxicity testing but are too large to fit inside narrow capillaries).[10,40–42]
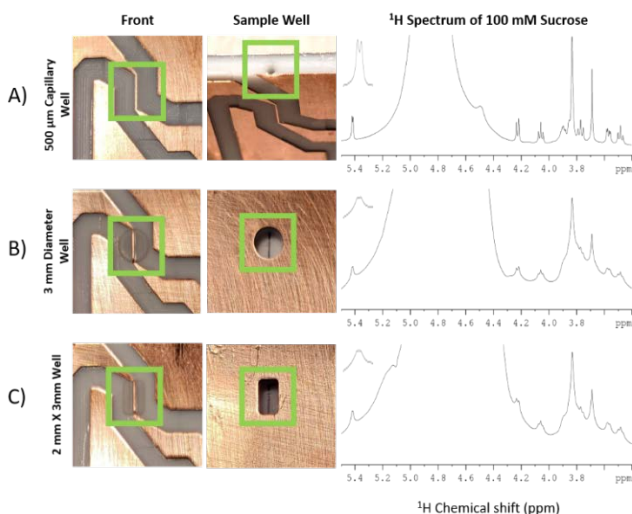
Figure 3. Three 3 mm long and 150 µm wide microstrips were milled each with different sample well geometries (left). Capillary (A), circular (B), and rectangular (C) well geometries are shown. The green boxes highlight the microstrip regions (left column), and the sample wells (middle column). Each microstrip was used to analyse a 100 mM Sucrose solution in H_2O (right, 256 scans).

Figure S2 shows the nutation curves for different sample wells. In the case of the capillary well, as the sample is restricted within the more homogeneous region at the microstrip surface the capillary design shows the best nutation curve (i.e. shorter 90° pulse and improved inversion).[19,34,39,43] However, the nutation curve is far from ideal, explained by the fact the capillary used here is 0.5 mm in diameter over a microstrip that is only 150 µm wide. The nutation curves for the round and rectangular wells are even worse as their larger sample size lead to an even smaller percentage of the sample being within the region close to the microstrip surface that receives a more homogeneous B_1 field.

One limitation for micro-drilling the capillary for the sample well is that there is a limit on the length/width ratio of the micro drill bits that are available. For example, at Performance Micro Tool the longest available 300 µm diameter wide bit is only 7.1 mm long and the longest available 150 µm diameter wide bit is only 3 mm long. As such, there are some restrictions for drilling very long thin capillaries. Other options could be to 1) drill the capillary as a "channel" from the rear, 2) or in some cases (dimensions permitting), use a longer and wider bit to open up access to the sample location and then use the fine bit to form the sample well. With the caveats noted, the versatility from forming the coil and sample well at the same time allows for the optimization of specific sample geometries as needed. This is important as matching the sample size and geometry of the well/coil is critical and can increase mass sensitivity by many orders of magnitude for microscopic samples vs. using off the shelf standard 5 mm NMR probes.[19]

Microstrip Optimization for *D. magna*. When developing micro-coil NMR, researchers often have target samples in mind. In the case of intact biological samples, these have a predefined sample size and shape. In aquatic toxicity studies, *D. magna* are the most commonly studied organisms.[40–42] Due to the magnetic susceptibility broadening in the ^{1}H NMR, 2D [1]H-^{13}C is often used in combination with ^{13}C enrichment for both *ex vivo* and *in vivo* metabolic profiling in *Daphnia*.[11–14,44,45] Commonly, for such studies 20 adult *Daphnia* are used in a 5 mm flow cryoprobe system.[11] However, given that ^{13}C enrichment of whole organisms is very expensive and *in vivo* exposure trajectories need to be repeated numerous times (including controls) for statistical analysis[11] studies require large cultures that are both challenging and expensive to maintain. However, if metabolic screening could be performed using fewer organisms using micro-coil NMR it drastically reduces the cost critical to implement *in vivo* toxicity screening on a routine basis. As adult *Daphnia* are around 1.5-2 mm in diameter, a 4 mm x 2 mm well was chosen to accommodate two adult organisms. In turn, given the high sensitivity of microstrips[34] and the fact they match well with elongated samples they were chosen for experimental optimization. Note the goal is not to design the absolute best coil for *D. magna* per se, but instead demonstrate how micro-milling can be used to rapidly prototype coil geometry given a fixed sample size and coil design.
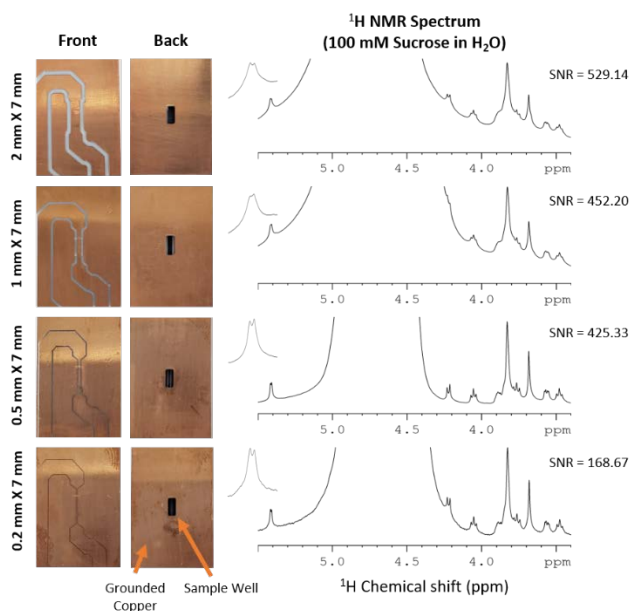

Figure 4. Four 7 mm long microstrip prototypes were produced each containing a 2 mm x 4 mm well (large enough to hold two *D. magna* organisms). The SNR for the sucrose signals (3-4 ppm) are reported (32 scans).

Figure 4 shows four different microstrips over a consistent sample well (all with a 2 mm width, a 4 mm length, and 1.58 mm depth). The length of the strip was set to 7 mm and the copper on the back was grounded to allow the RF to penetrate further into the sample.[34] The width of the strip was varied for each microstrip (2 mm,

1 mm, 0.5 mm and 0.2 mm) with the spacing around the strip set at half the strip width. While a smaller gap width reduces susceptibility distortions, it also reduces sensitivity because the magnetic field lines have to squeeze closer together, causing larger eddy currents and thus losses. Therefore, as the strip lines are scaled down, the percentage of losses due to these eddy currents, as well as the line width (B_0), will remain the same. A ratio of half of the strip width was used to be consistent with previous studies[27,46] which identified this ratio to be a good compromise between sensitivity and resolution for ^{1}H spectroscopy.

All B_1 field simulations for these microstrips are shown in Figure S3. While the B_1 field for wider microstrips penetrate further into the sample, the narrower microstrips produce a more intense localized B_1 field close to the surface as such it is hard to predict exactly from simulations which will give most signal in the relatively large sample well required to accommodate two *Daphnia*.

Experimental ^{1}H NMR results show that the largest 2 mm strip indeed provided the highest SNR for the set sample size but only ~17% more than the 1 mm strip with the 500 µm strip not far behind. The smaller strips (500 µm and 200 µm) produce improved lineshape due to improved shimming in the smaller excited region. Figure S4 shows the nutation curves improve as the strip width increases due to more of the sample being uniformly excited.[19] As such, from ^{1}H NMR data and simulations alone the 2 mm strip (which matches the sample well width) would be the obvious choice. However, in practice when double tuned and used for a [1]H-^{13}C HMQC it was found that the 2 mm microstrip required >100 W for the adiabatic inversion on the ^{13}C channel vs. only 27 W for the 1 mm microstrip. Considering the probe body is a prototype provided by Bruker without peak RF handling limits, it was decided to err on the side of caution and use the 1 mm design rather than the 2 mm design for the analysis of *D. magna*. This result is interesting as it demonstrates that while simulations and precedent[19] suggest matching the coil size to the sample will give optimal signal, the ability to quickly and affordably build prototypes can provide key practical insights that are hard to predict. This is especially important given that micro-coils are traditionally manufactured using multilayer technologies in dedicated clean rooms that can be very expensive and take months to complete.[20,29] In comparison, here it was possible to design, mill, and match/tune a microstrip within 24 hrs once the process was optimized.
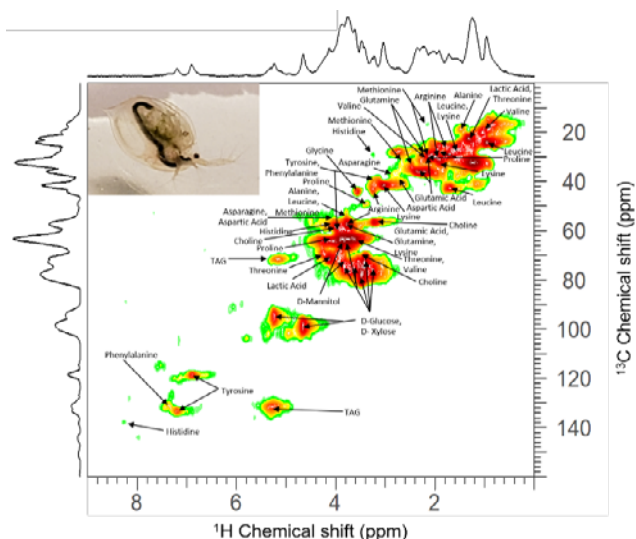

Figure 5. Two uniformly ^{13}C-labelled *D. magna* adults were analysed using the optimized microstrip design. A total of 22 metabolites were able to be identified using Bruker's Bioreference Software Database. Results from a study by Fortier-McGill *et al.*[47] was used to identify Triglycerides (TAG). A photo of a *D. magna* adult is also shown.

Figure 5 shows a [1]H-^{13}C HMQC of two intact ^{13}C-labelled adult *D. magna* acquired using the 1 mm x 7 mm microstrip. The organisms were placed into the holder alive but died during the 16 hr analysis. In the future, flow capabilities should be integrated into the micro-coil designs in order to supply the organisms with food and oxygen to keep them alive.[11] However, the results are highly encouraging, and a range of metabolites can still be assigned from only two *Daphnia* (~200 µg dry weight). Indeed, the number of signals and metabolites are very similar to those identified using 5 mm cryoprobes and using 10 times as many organisms.[14,15] As such, it is clear micro-milled micro-coils perform very well and have practical applications for mass limited samples.

Volume vs. Surface Coils. Thus far all the coils made are two-dimensional and can be manufactured using only a 3-axis milling machine (i.e. X/Y/Z movements). However, it is also feasible to make 3D volume coils if all 5 axes (X/Y/Z/A/B) are used. To the authors' knowledge to date, the best balance between mass and concentration sensitivity was achieved by Finch *et al.*[27] using a double stripline design. Here, the idea was adapted but instead of making the pieces as separate parts and then constructing the 3D device in layers, the device was machined as a single piece such that it roughly resembles a slotted tube resonator (STR).[35,48] For simplicity, the resonator was milled from a copper tube, but could be machined from a solid copper rod (or block) if required.
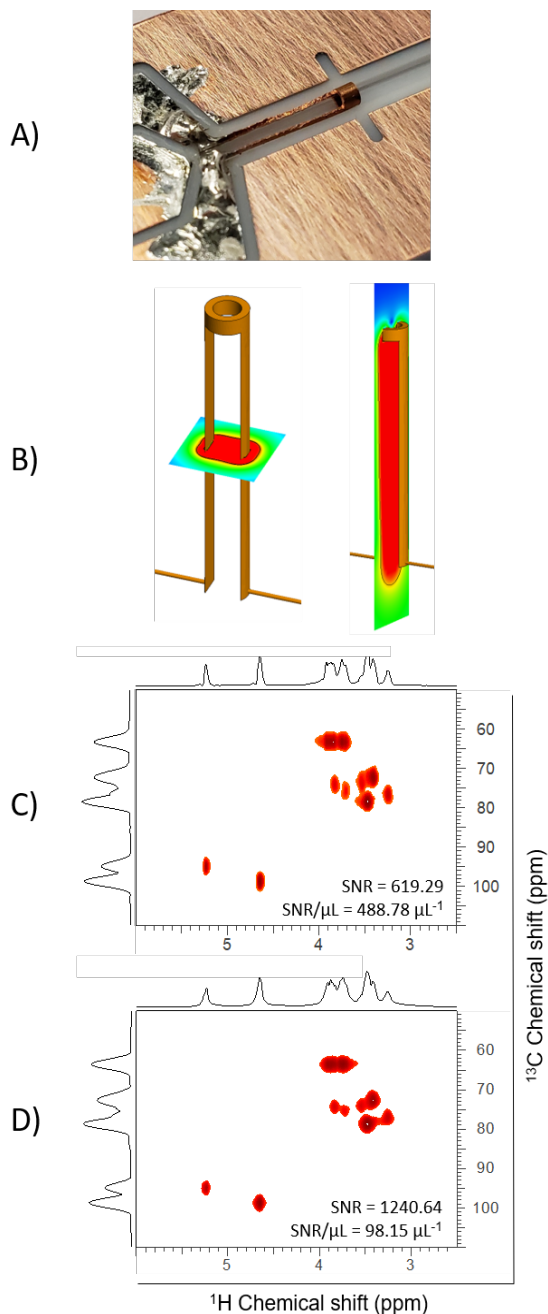
Figure 6. An STR (A) was produced with the intention of analysing mass-limited biological samples. A CAD drawing of the STR (with the B_1 profiles produced using Feko) is also shown (B). The black contour represents the 90% RF field lines for the STR. HMQC experiments were performed on a 1 M ^{13}C-D-Glucose solution (in D$_2$O) using both the STR (C) and the previously described 1 mm X 7 mm microstrip (D). The resulting spectra closely resembled what was provided by the Bruker Bioreference database. For the microstrip, the sample was contained in a 2 mm x 4 mm x 1.58 mm well while the sample for the STR was contained within a glass capillary with a 500 μm O.D. and 10 μm glass walls.

Similar to the Finch *et al.*[27] design, the B_1 field between the two plates is highly concentrated and uniform between the plates. As such, the nutation curve produced by the resonator provides improved inversion important for 2D NMR (Figure S5). In turn, the SNR per

μL of sample produced in ^{1}H-^{13}C HMQC is excellent and increases 5-fold over the single sided microstrip (see Figure 6). This is predominantly explained by the complete and uniform penetration of the B_1 field throughout the sample for the slotted resonator design (a comparison of the B_1 profiles for the two micro-sensors is shown in Figure S6). In a previous study it was shown that 80% of the signal was lost when complex multiple pulse experiments were applied to single sided surface coils due to RF inhomogeneity.[19] Indeed a similar value of 80% loss was observed here for the sample run on the single sided microstrip vs. the STR.

Sensitivity Comparison. Arguably the most practical NMR micro-sensor published to date is the double stripline design by Finch *et al.*[27], which shows the best combination of concentration sensitivity and mass sensitivity to date. Following the method for measuring sensitivity outlined by Finch *et al.*[27], 150 mM Sodium Acetate was used as a test sample. Figure S7 shows an SNR of 49.9 was achieved for a 20 nL sample contained within an 80 μm I.D. diameter capillary (4 mm sample height). When the different fields (300 MHz by Finch *et al.*[27] and 500 MHz in this study) are accounted for and a loss of 50% factored in for the double tuned (^{1}H-^{13}C) circuit used here vs. the single tuned ^{1}H only circuit[49] used by Finch *et al.*[27], the sensitivity of the STR described is on par with its previous counterpart. When converted to a field strength of 600 MHz which is common practice to permit micro-coil comparison[27] this gives a detection limit nLOD$_\Omega^{600}$= 1.49 nmol s$^{1/2}$ for the STR described here. However, it is still behind the most recently reported value by Sharma and Utz[46] of 1.40 nmol s$^{1/2}$ for ^{1}H on a double stripline resonator mounted on a specially designed transmission line probe. The improved sensitivity achieved by Sharma and Utz[46] is likely in part due to their optimal transmission probe design and in part due to the reduced lineshape of the STR described here.

Figure S8 shows an expansion of the acetate peak, while it has reasonable linewidth at half height (~0.015 ppm) it has a slight asymmetry that cannot be shimmed away, which will impact SNR measurements that are based on peak height. For a wider capillary (680 μm I.D.) the situation becomes worse (see Figure S8B). In this case, as the sample is brought close to the surface of the copper the magnetic susceptibility differences between the sample, glass, and copper lead to distorted magnetic environments and poor lineshape. To avoid this, Finch *et al.*[27] used acrylic for the sample holder and printed circuit boards with only 18 μm thick copper layers which produced a more homogeneous magnetic environment and superior lineshape. The advantage of 5-axis milling is that if sensors can be machined directly from metal blocks then sensors of virtually any size, shape, or complexity can be easily manufactured. A viable future solution to reduce magnetic susceptibility distortions could be to machine the parts from aluminium, which has a positive magnetic susceptibility, and then electroplate

with copper that has a negative susceptibility. At the ideal ratio, the susceptibilities should cancel leading to zero distortions form the coil materials. Indeed, a similar approach was successfully demonstrated for NMR micro-coils which used layered aluminium/copper "zero" susceptibility wire.[24]

Testing the Slotted-Tube Resonator on *D. magna* Neonates. While fully dissolved solutions of simple chemicals can give rise to sharp lines, intact biological samples such as small organisms and eggs themselves distort the applied B_0 field leading to broad lineshape often in the range on 0.1-0.2 ppm at 500 MHz for *Daphnia*.[9] As such, as long as the magnetic susceptibilities from the coil are not much larger than those produced by the natural samples themselves, then the impact of coil induced spectral broadening is greatly reduced for intact samples with naturally broad lineshape.

To demonstrate that the STR has applications even in its current form for biological samples, it was tested on 14 freeze-dried ^{13}C-labelled *D. magna* neonates (1-2 days old). With a dry weight of ~1.5 µg,[50] this represents ~20 µg and 1/10th of the dry weight analysed in the two adult *Daphnia* on the microstrip. While the SNR is relatively low, a range of metabolites can still be identified (shown in Figure 7). In addition to the expected amino acids, additional products of carbohydrate and glycerol metabolism by microorganisms (such as acetaldehyde, acetic acid, 1-butanol, ethanol, 1,2-propanediol and 1,3-propanediol) were also present within the sample.[51–55]
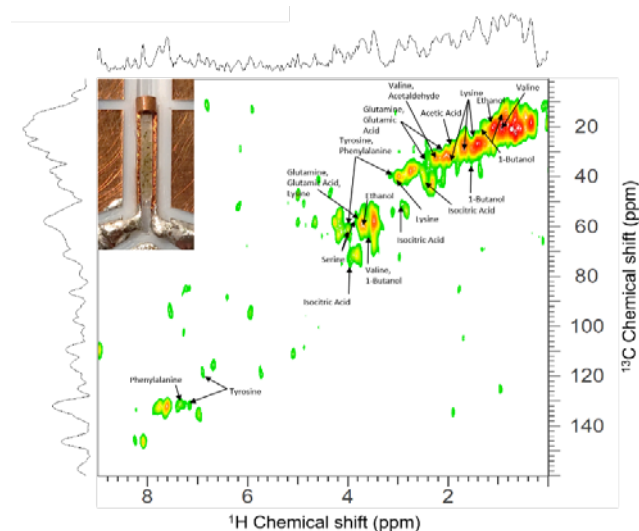

Figure 7. The milled STR was used to analyse 14 *D. magna* neonates in a glass capillary with a 700 µm O.D. and 10 µm walls. A total of 12 metabolites were able to be identified using Bruker's Bioreference Software Database. The *D. magna* neonates inside the STR are also shown.

In a paper by Dutta Majumdar *et al.*[15] 100 *D. magna* neonates were needed to provide a usable 1D ^{1}H NMR signal using a Bruker 5 mm QXI probe. The signal however was still much smaller than that from 10 adults and 2D ^{1}H-^{13}C NMR was not attempted in the Dutta Majumdar *et al.*[15] study. Here, using the milled STR only 14 neonates were needed to obtain a usable amount of signal in 2D ^{1}H-^{13}C NMR and represent to our knowledge the first 2D NMR of *Daphnia* neonates.

In summary, this demonstrates that the milled resonators have considerable potential and even the early prototypes described here are nearly as sensitive as the most practical resonators published to date[27,46] and open up the door for novel NMR of mass-limited biological samples.

CONCLUSIONS

In this study, we demonstrated CNC micro-milling can produce working planar micro-coils, microstrips, and other micro-sensor designs. In addition, sample wells can also be easily constructed and optimized according to the sample type and the micro-sensor type. In turn this demonstrates the versatility of 5-axis CNC micro-milling as a rapid prototyping technique for manufacturing NMR micro-sensors. Furthermore, the prototype 1 mm x 7 mm microstrip and 3D volume STR were successfully applied to collect 2D ^{1}H-^{13}C NMR on two adult *D. magna* (~200 µg) and 14 neonates (~20 µg), respectively. The STR showed an SNR within the same ballpark of arguably the most practical micro-sensors published to date for mass limited biological samples.[27,46] Future work will focus on reducing the magnetic susceptibility of the STR via plating or the use of alloys.

Overall, this study is the first thorough demonstration of the capabilities of 5-axis CNC micro-milling as a technique for rapid and economic production of micro-coil and micro-sensor technology for NMR. The machines are extremely versatile and are commonly used for the highest resolution molds in the jewelry industry, as such they can be used to generate highly intricate models.[56] As such, in future, it should be possible to generate all sorts of volume NMR coils, such as saddles, solenoids, birdcages, Helmholtz etc. if needed. The main limitation, is the aspect ratio of the smallest (<100 µm) milling bits that tend to have only ~3:1 (length: depth, i.e. a 100 µm bit can only mill 300 µm deep). However, assuming thin walled metal capillaries can be purchased, or long aspect ratio drilling bits (drilling bits drill only vertically and often have aspect ratios >20:1) used to hollow out rods, then it should be possible to mill practically any pattern into the tube walls and thus generate all common types of NMR coils and protype novel designs.

ASSOCIATED CONTENT

Supporting Information

The Supporting Information is available free of charge on the ACS Publications website and contains nutation curves and peak expansions referred to from the main text.

AUTHOR INFORMATION

Corresponding Author

*Corresponding Author: andre.simpson@utoronto.ca

Author Contributions

The manuscript was written through contributions of all authors. All authors have given approval to the final version of the manuscript.

ACKNOWLEDGMENT

REFERENCES

(1) Campbell, A. Inflammation, Neurodegenerative Diseases, and Environmental Exposures. *Ann. N. Y. Acad. Sci.* **2004**, *1035*, 117–132. https://doi.org/10.1196/annals.1332.008.

(2) Cannon, J. R.; Greenamyre, J. T. The Role of Environmental Exposures in Neurodegeneration and Neurodegenerative Diseases. *Toxicol. Sci.* **2011**, *124* (2), 225–250. https://doi.org/10.1093/toxsci/kfr239.

(3) Charlet, L.; Chapron, Y.; Faller, P.; Kirsch, R.; Stone, A. T.; Baveye, P. C. Neurodegenerative Diseases and Exposure to the Environmental Metals Mn, Pb, and Hg. *Coord. Chem. Rev.* **2012**, *256*, 2147–2163. https://doi.org/10.1016/j.ccr.2012.05.012.

(4) Parrón, T.; Requena, M.; Hernández, A. F.; Alarcón, R. Association between Environmental Exposure to Pesticides and Neurodegenerative Diseases. *Toxicol. Appl. Pharmacol.* **2011**, *256*, 379–385. https://doi.org/10.1016/j.taap.2011.05.006.

(5) Simpson, A. J.; Liaghati, Y.; Fortier-Mcgill, B.; Soong, R.; Akhter, M. Perspective: In Vivo NMR - A Potentially Powerful Tool for Environmental Research. *Magn. Reson. Chem.* **2015**, *53*, 686–690. https://doi.org/10.1002/mrc.4142.

(6) Schwarzenbach, R. P.; Escher, B. I.; Fenner, K.; Hofstetter, T. B.; Johnson, C. A.; von Gunten, U.; Wehrli, B. The Challenge of Micropollutants in Aquatic Systems. *Science (80-.).* **2006**, *313*, 1072–1077.

(7) Little, E. E.; Archeski, R. D.; Flerov, B. A.; Kozlovskaya, V. I. Behavioral Indicators of Sublethal Toxicity in Rainbow Trout. *Arch. Environ. Contam. Toxicol.* **1990**, *19*, 380–385.

(8) Bastawrous, M.; Jenne, A.; Tabatabaei Anaraki, M.; Simpson, A. J. In-Vivo NMR Spectroscopy : A Powerful and Complimentary Tool for Understanding Environmental Toxicity. *Metabolites* **2018**, *8* (35), 1–24. https://doi.org/10.3390/metabo8020035.

(9) Fugariu, I.; Bermel, W.; Lane, D.; Soong, R.; Simpson, A. J. In-Phase Ultra High-Resolution In Vivo NMR. *Angew. Chemie - Int. Ed.* **2017**, *56* (22), 6324–6328. https://doi.org/10.1002/anie.201701097.

(10) Liaghati Mobarhan, Y.; Fortier-McGill, B.; Soong, R.; Maas, W. E.; Fey, M.; Monette, M.; Stronks, H. J.; Schmidt, S.; Heumann, H.; Norwood, W.; et al. Comprehensive Multiphase NMR Applied to a Living Organism. *Chem. Sci.* **2016**, *7*, 4856–4866. https://doi.org/10.1039/C6SC00329J.

(11) Tabatabaei Anaraki, M.; Dutta Majumdar, R.; Wagner, N.;

(12) Soong, R.; Kovacevic, V.; Reiner, E. J.; Bhavsar, S. P.; Ortiz Almirall, X.; Lane, D.; Simpson, M. J.; et al. Development and Application of a Low-Volume Flow System for Solution-State in Vivo NMR. *Anal. Chem.* **2018**, *90*, 7912–7921. https://doi.org/10.1021/acs.analchem.8b00370.

(12) Tabatabaei Anaraki, M.; Simpson, M. J.; Simpson, A. J. Reducing Impacts of Organism Variability in Metabolomics via Time Trajectory in Vivo NMR. *Magn. Reson. Chem.* **2018**, *56* (May), 1117–1123. https://doi.org/10.1002/mrc.4759.

(13) Lane, D.; Skinner, T. E.; Gershenzon, N. I.; Bermel, W.; Soong, R.; Dutta Majumdar, R.; Liaghati, Y.; Sebastian, M.; Hermann, S.; Monette, M.; et al. Assessing the Potential of Quantitative 2D HSQC NMR in 13C Enriched Living Organisms. *J. Biomol. NMR* **2019**, *73*, 31–42. https://doi.org/10.1007/s10858-018-0221-2.

(14) Soong, R.; Nagato, E.; Sutrisno, A.; Fortier-Mcgill, B.; Akhter, M.; Schmidt, S.; Heumann, H.; Simpson, A. J. In Vivo NMR Spectroscopy: Toward Real Time Monitoring of Environmental Stress. *Magn. Reson. Chem.* **2015**, *53*, 774–779. https://doi.org/10.1002/mrc.4154.

(15) Dutta Majumdar, R.; Akhter, M.; Fortier-McGill, B.; Soong, R.; Liaghati-Mobarhan, Y.; Simpson, A. J.; Spraul, M.; Schmidt, S.; Heumann, H. In Vivo Solution-State NMR-Based Environmental Metabolomics. *eMagRes* **2017**, *6*, 133–148. https://doi.org/10.1002/9780470034590.emrstm1533.

(16) Miner, B. E.; De Meester, L.; Pfrender, M. E.; Lampert, W.; Hairston, N. G. Linking Genes to Communities and Ecosystems: Daphnia as an Ecogenomic Model. *Proc. R. Soc. B* **2012**, *279*, 1873–1882. https://doi.org/10.1098/rspb.2011.2404.

(17) Hairston, N. G. Zooplankton Egg Banks as Biotic Reservoirs in Changing Environments. *Limnol. Ocean.* **1996**, *41* (5), 1087–1092.

(18) Wagner, N. D.; Simpson, A. J.; Simpson, M. J. Metabolomic Responses to Sublethal Contaminant Exposure in Neonate and Adult Daphnia Magna. *Environ. Toxicol. Chem.* **2017**, *36* (4), 938–946. https://doi.org/10.1002/etc.3604.

(19) Fugariu, I.; Soong, R.; Lane, D.; Fey, M.; Maas, W.; Vincent, F.; Beck, A.; Schmidig, D.; Treanor, B.; Simpson, A. J. Towards Single Egg Toxicity Screening Using Microcoil NMR. *Analyst* **2017**, *142* (24), 4812–4824. https://doi.org/10.1039/c7an01339f.

(20) Massin, C.; Boero, G.; Vincent, F.; Abenhaim, J.; Besse, P. A.; Popovic, R. S. High-Q Factor RF Planar Microcoils for Micro-Scale NMR Spectroscopy. *Sensors Actuators, A Phys.* **2002**, *97–98*, 280–288. https://doi.org/10.1016/S0924-4247(01)00847-0.

(21) Ehrmann, K.; Saillen, N.; Vincent, F.; Stettler, M.; Jordan, M.; Wurm, F. M.; Besse, P.-A.; Popovic, R. Microfabricated Solenoids and Helmholtz Coils for NMR Spectroscopy of Mammalian Cells. *Lab Chip* **2007**, *7*, 373–380. https://doi.org/10.1039/b614044k.

(22) Spengler, N.; Höfflin, J.; Moazenzadeh, A.; Mager, D.; MacKinnon, N.; Badilita, V.; Wallrabe, U.; Korvink, J. G. Heteronuclear Micro-Helmholtz Coil Facilitates Mm-Range Spatial and Sub-Hz Spectral Resolution NMR of NL-Volume Samples on Customisable Microfluidic Chips. *PLoS One* **2016**, *11* (1), 1–16. https://doi.org/10.1371/journal.pone.0146384.

(23) Subramanian, R.; Webb, A. G. Design of Solenoidal Microcoils for High-Resolution 13C NMR Spectroscopy. *Anal. Chem.* **1998**, *70*, 2454–2458. https://doi.org/10.1021/ac980299s.

(24) Kc, R.; Henry, I. D.; Park, G. H. J.; Aghdasi, A.; Raftery, D. New Solenoidal Microcoil NMR Probe Using Zero-Susceptibility Wire. *Concepts Magn. Reson. Part B* **2010**, *37B* (1), 13–19. https://doi.org/10.1002/cmr.b.20152.New.

(25) Olson, D. L.; Lacey, M. E.; Sweedler, J. V. High-Resolution Microcoil NMR for Analysis of Mass-Limited, Nanoliter Samples. *Anal. Chem.* **1998**, *70*, 645–650. https://doi.org/10.1021/ac970972y.

(26) Jasiński, K.; Młynarczyk, A.; Latta, P.; Volotovskyy, V.; Weglarz, W. P.; Tomanek, B. A Volume Microstrip RF Coil for MRI Microscopy. *Magn. Reson. Imaging* **2012**, *30*, 70–77. https://doi.org/10.1016/j.mri.2011.07.010.

(27) Finch, G.; Yilmaz, A.; Utz, M. An Optimised Detector for In-Situ High-Resolution NMR in Microfluidic Devices. *J. Magn. Reson.* **2016**, *262*, 73–80. https://doi.org/10.1016/j.jmr.2015.11.011.

(28) Zhang, X.; Ugurbil, K.; Chen, W. Microstrip RF Surface Coil Design for Extremely High-Field MRI and Spectroscopy. *Magn. Reson. Med.* **2001**, *46*, 443–450.

https://doi.org/10.1002/mrm.1212.

(29)   Swyer, I.; Soong, R.; Dryden, M. D. M.; Fey, M.; Maas, W. E.; Simpson, A.; Wheeler, A. R. Interfacing Digital Microfluidics with High-Field Nuclear Magnetic Resonance Spectroscopy. *Lab Chip* **2016**, *16*, 4424–4435. https://doi.org/10.1039/C6LC01073C.

(30)   Massin, C.; Vincent, F.; Homsy, A.; Ehrmann, K.; Boero, G.; Besse, P. A.; Daridon, A.; Verpoorte, E.; de Rooij, N. F.; Popovic, R. S. Planar Microcoil-Based Microfluidic NMR Probes. *J. Magn. Reson.* **2003**, *164* (2), 242–255. https://doi.org/10.1016/S1090-7807(03)00151-4.

(31)   Wang, N.; Meissner, M. V.; MacKinnon, N.; Luchnikov, V.; Mager, D.; Korvink, J. G. Fast Prototyping of Microtubes with Embedded Sensing Elements Made Possible with an Inkjet Printing and Rolling Process. *J. Micromechanics Microengineering* **2018**, *28*, 1–10. https://doi.org/10.1088/1361-6439/aa7a61.

(32)   Liu, W.; Lu, L.; Mitrović, V. F. Application of Surface Coil for Nuclear Magnetic Resonance Studies of Semi-Conducting Thin Films. *Rev. Sci. Instrum.* **2017**, *88*, 1–7. https://doi.org/10.1063/1.4986047.

(33)   Fratila, R. M.; Gomez, M. V.; Sýkora, S.; Velders, A. H. Multinuclear Nanoliter One-Dimensional and Two-Dimensional NMR Spectroscopy with a Single Non-Resonant Microcoil. *Nat. Commun.* **2014**, *5*, 3025. https://doi.org/10.1038/ncomms4025.

(34)   Chen, Y.; Mehta, H. S.; Butler, M. C.; Walter, E. D.; Reardon, P. N.; Renslow, R. S.; Mueller, K. T.; Washton, N. M. High-Resolution Microstrip NMR Detectors for Subnanoliter Samples. *Phys. Chem. Chem. Phys.* **2017**, *19*, 28163–28174. https://doi.org/10.1039/c7cp03933f.

(35)   Benabdallah, N.; Benahmed, N.; Benyoucef, B.; Bouhmidi, R.; Khelif, M. Electromagnetic Analysis of the Slotted-Tube Resonator with a Circular Cross Section for MRI Applications. *Phys. Med. Biol.* **2007**, *52*, 4943–4952. https://doi.org/10.1088/0031-9155/52/16/015.

(36)   Krojanski, H. G.; Lambert, J.; Gerikalan, Y.; Suter, D.; Hergenröder, R. Microslot NMR Probe for Metabolomics Studies. *Anal. Chem.* **2008**, *80* (22), 8668–8672. https://doi.org/10.1021/ac801636a.

(37)   van Meerten, S. G. J.; van Bentum, P. J. M.; Kentgens, A. P. M. Shim-on-Chip Design for Microfluidic NMR Detectors. *Anal. Chem.* **2018**, *90*, 10134–10138. https://doi.org/10.1021/acs.analchem.8b02284.

(38)   Gladysz, J. A.; Jurisch, M. *Structural, Physical, and Chemical Properties of Fluorous Compounds*; Horvath, I. T., Ed.; Springer-Verlag: Berlin Heidelberg, 2012; Vol. 308.

(39)   Chmurny, G. N.; Hoult, D. I. The Ancient and Honourable Art of Shimming. *Concepts Magn. Reson.* **1990**, *2*, 131–149.

(40)   Janssen, C. R.; Persoone, G. Rapid Toxicity Screening Tests for Aquatic Biota. 1. Methodology and Experiments with Daphnia Magna. *Environ. Toxicol. Chem.* **1993**, *12*, 711–717.

(41)   Kovacevic, V.; Simpson, A. J.; Simpson, M. J. 1H NMR-Based Metabolomics of Daphnia Magna Responses after Sub-Lethal Exposure to Triclosan, Carbamazepine and Ibuprofen. *Comp. Biochem. Physiol. Part D* **2016**, *19*, 199–210. https://doi.org/10.1016/j.cbd.2016.01.004.

(42)   Nagato, E. G.; D'eon, J. C.; Lankadurai, B. P.; Poirier, D. G.; Reiner, E. J.; Simpson, A. J.; Simpson, M. J. 1H NMR-Based Metabolomics Investigation of Daphnia Magna Responses to Sub-Lethal Exposure to Arsenic, Copper and Lithium. *Chemosphere* **2013**, *93*, 331–337. https://doi.org/10.1016/j.chemosphere.2013.04.085.

(43)   Haase, A.; Odoj, F.; von Kienlin, M.; Warnking, J.; Fidler, F.; Weisser, A.; Nittka, M.; Rommel, E.; Lanz, T.; Kalusche, B.; et al. NMR Probeheads for in Vivo Applications. *Concepts Magn. Reson.* **2000**, *12* (6), 361–388. https://doi.org/10.1002/1099-0534(2000)12:6<361::AID-CMR1>3.0.CO;2-L.

(44)   Tabatabaei Anaraki, M.; Bermel, W.; Dutta Majumdar, R.; Soong, R.; Simpson, M.; Monnette, M.; Simpson, A. J. 1D "Spikelet" Projections from Heteronuclear 2D NMR Data—Permitting 1D Chemometrics While Preserving 2D Dispersion. *Metabolites* **2019**, *9* (16), 1–11. https://doi.org/10.3390/metabo9010016.

(45)   Jenne, A.; Soong, R.; Bermel, W.; Sharma, N.; Masi, A.; Tabatabaei Anaraki, M.; Simpson, A. Focusing on "the Important" through Targeted NMR Experiments: An Example of Selective 13 C– 12 C Bond Detection in Complex Mixtures . *Faraday Discuss.* **2019**, *218*, 372–394. https://doi.org/10.1039/c8fd00213d.

(46)   Sharma, M.; Utz, M. Modular Transmission Line Probes for Microfluidic Nuclear Magnetic Resonance Spectroscopy and Imaging. *J. Magn. Reson.* **2019**, *303*, 75–81. https://doi.org/10.1016/j.jmr.2019.04.007.

(47)   Fortier-McGill, B. E.; Dutta Majumdar, R.; Lam, L.; Soong, R.; Liaghati-mobarhan, Y.; Sutrisno, A.; Visser, R. De; Simpson, M. J.; Wheeler, H. L.; Campbell, M.; et al. Comprehensive Multiphase (CMP) NMR Monitoring of the Structural Changes and Molecular Flux Within a Growing Seed. *J. Agric. Food Chem.* **2017**, *65*, 6779–6788. https://doi.org/10.1021/acs.jafc.7b02421.

(48)   Nespor, D.; Bartusek, K.; Dokoupil, Z. Comparing Saddle, Slotted-Tube and Parallel-Plate Coils for Magnetic Resonance Imaging. *Meas. Sci. Rev.* **2014**, *14* (3), 171–176. https://doi.org/10.2478/msr-2014-0023.

(49)   Fitzsimmons, J. R.; Brooker, H. R.; Beck, B. A Comparison of Double-tuned Surface Coils. *Magn. Reson. Med.* **1989**, *10*, 302–309. https://doi.org/10.1002/mrm.1910100303.

(50)   Wagner, N. D.; Lankadurai, B. P.; Simpson, M. J.; Simpson, A. J.; Frost, P. C. Metabolomic Differentiation of Nutritional Stress in an Aquatic Invertebrate. *Physiol. Biochem. Zool.* **2015**, *88* (1), 43–52. https://doi.org/10.1086/679637.

(51)   Udaondo, Z.; Ramos, J. L.; Segura, A.; Krell, T.; Daddaoua, A. Regulation of Carbohydrate Degradation Pathways in Pseudomonas Involves a Versatile Set of Transcriptional Regulators. *Microb. Biotechnol.* **2018**, *11*, 442–454. https://doi.org/10.1111/1751-7915.13263.

(52)   Romano, P.; Fiore, C.; Paraggio, M.; Caruso, M.; Capece, A. Function of Yeast Species and Strains in Wine Flavour. *Int. J. Food Microbiol.* **2003**, *86*, 169–180. https://doi.org/10.1016/S0168-1605(03)00290-3.

(53)   Nissen, T. L.; Kielland-Brandt, M. C.; Nielsen, J.; Villadsen, J. Optimization of Ethanol Production in Saccharomyces Cerevisiae by Metabolic Engineering of the Ammonium Assimilation. *Metab. Eng.* **2000**, *2*, 69–77. https://doi.org/10.1006/mben.1999.0140.

(54)   Saxena, R. K.; Anand, P.; Saran, S.; Isar, J.; Agarwal, L. Microbial Production and Applications of 1,2-Propanediol. *Indian J. Microbiol.* **2010**, *50* (1), 2–11. https://doi.org/10.1007/s12088-010-0017-x.

(55)   Biebl, H.; Menzel, K.; Zeng, A. P.; Deckwer, W. D. Microbial Production of 1 , 3-Propanediol. *Appl. Microbiol. Biotechnol.* **1999**, *52*, 289–297.

(56)   NS CNC. Photo Gallery https://nscnc.com/photo-gallery/.